Propagation of Elastic Waves in Nanostructures

S. Gopalakrishnan*[a]

[a] Department of Aerospace Engineering, Indian Institute of Science, Bangalore 560012, India

ABSTRACT

This paper presents the study of propagation of elastic waves in nano structures using continuum approximation. The wave propagation characteristics in both 1-D and 2-D nanostructures, namely the carbon nanotubes and Graphene are studied in this paper. In particular, the use of various gradient elasticity theories, namely the Eringen's Stress gradient theory, the second and fourth order strain gradient theories, that brings in atomistic length scale parameters into the continuum governing equations, is used in this paper to study the wave propagation characteristics in the nano structures. Using these non-local theories, wave propagation in Single and Multi-wall carbon tubes and monolayer Graphene structures are studied. A number of examples are presented that brings out the essential wave propagation features such as escape frequency, cut-off frequencies, phase speeds and group speeds in these structures.

Keywords: Nanostructures, carbon nanotubes, Graphene, wavenumber, group speeds, escape frequency, cut-off frequency.

1. INTRODUCTION

Mathematical modeling of structures at the micro and macroscales are quite well known and the methods have been well established. The laws of physics, which is fundamental to any modeling, is pretty well understood at these scales. At the nano meter levels, we need to deal with atoms, molecules and their interactions. The laws of physics, at these scales, are not that well understood. The main difference lies in representing the models in different scales. That is, the philosophies of modeling at different scales are different. At the nano scales, forces have no meaning, while at the micro and macro scales, they are the main drivers. At the nano scales, it is the *interatomic potentials*[1] that plays an important part in understanding the behavior of the nanostructures. A number of different inter atomic potentials have been propounded by many scientists for different conditions and the reference[1] gives a good overview of these potentials. It is quite well known that one can modify the bulk properties of the material by manipulating the atoms and molecules at the nano scales. That is, using the inter atomic potentials and the laws of physics at the nano scales, one has to predict the bulk properties such as phase information, structural property information etc as illustrated in Fig. 1

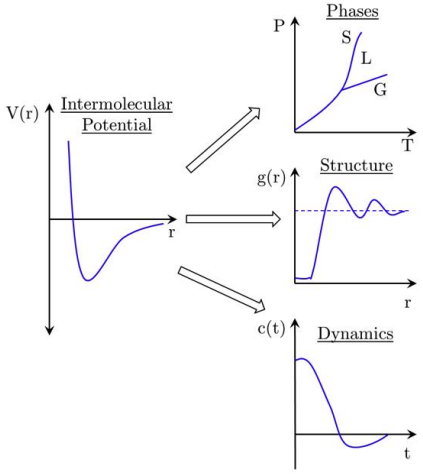

Figure 1. Simulations as a bridge between microscopic and macroscopic.

*krishnan@aero.iisc.ernet.in; phone 91 80 2293 3019; fax 91 80 23604551; www.aero.iisc.ernet.in/users/gopalkrishnan

Nanosensors, Biosensors, and Info-Tech Sensors and Systems 2016,
edited by Vijay K. Varadan, Proc. of SPIE Vol. 9802, 98020N · © 2016
SPIE · CCC code: 0277-786X/16/$18 · doi: 10.1117/12.2218203

The most common approach to materials modeling is based on the *divide and conquer* strategy, wherein methods appropriate to particular length and time scales are used to address aspects of materials phenomena that operate only over those scales. This has led to several independent methodological streams, which can be broadly categorized as *ab initio* density functional theory, molecular dynamics, statistical methods based on Monte Carlo algorithms and continuum mechanics. Each of these methods is computationally intensive in its own right, and hence most of the initial efforts were directed in optimizing algorithms, potentials and parameters for each method individually, rather than generating information for input into other methods.

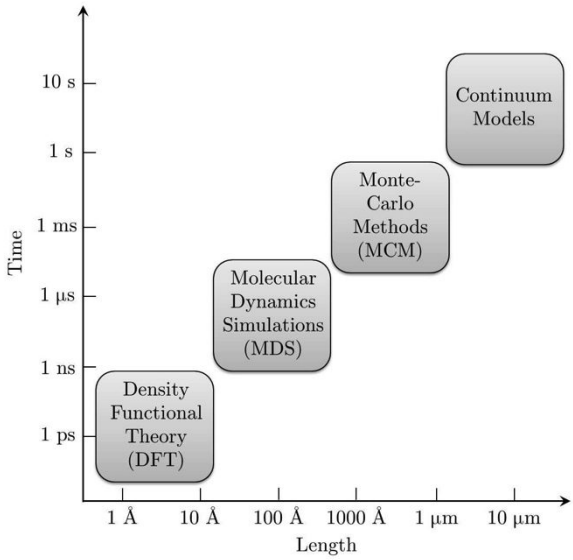

Figure 2. Different modeling schemes for various spatial scales.

The Fig. 3.2 clearly shows the length and time scales over which these methods are valid. However, the expanding capabilities of computational methods due to the increasing power of computers and continuing development of efficient algorithms, together with advances in the synthesis, analysis and visualization of materials at increasingly finer spatial and temporal resolutions, has spawned a huge effort in the Multiscale descriptions of materials phenomena.

Propagation of mechanical waves in macro-sized structures are normally studied using the concepts of elasticity. Most macrostructures such as rods, beams, plates and shells are studied using Theory of elasticity, which we normally refer to as ***Local theory.*** Nano structures are typically of *nano meter size* (1×10^{-9} m).

Unlike continuum model, which describe a system in terms of a few variables such as mass, temperature, voltage and stress, which are highly suited for direct measurements of these variables, the physical world is composed of atoms moving under the influence of their mutual interaction forces. Atomistic investigation helps to identify macroscopic quantities and their correlations, and enhance our understanding of various physical theories. In the new modeling philosophy, due to computationally expensive atomistic simulation, many researchers have tried to embed the micro level properties such as bond-lengths into the continuum theories. A theory, which embeds micro-structural properties into theory of elasticity or local theory is called the ***Non-local theory***. Among the many different non-local theories reported in the literature, *gradient elasticity* models are extensively used. There are two different gradient elasticity theories, namely the *Eringen's Stress Gradient Theory* and *Strain Gradient Theory*. These theories will be briefly discussed in this paper.

Next, we explain the need for wave propagation analysis in nanostructures. Controlled experiments at the nano meter size is extremely difficult, especially to measure mechanical properties of nano structures and devices. Hernaandez *et al.*[2] used high-frequency laser-excited guided acoustic waves to estimate the in-plane mechanical properties of silicon nitride membranes. Mechanical properties and residual stresses in the membranes were evaluated from measured acoustic

dispersion curves. The mean values of the Young's modulus and density of three Nano crystalline diamond films and a free standing diamond plate were determined by analyzing the dispersion of laser- generated surface waves by Philip *et al.*[3].

Nanostructures such as Carbon nanotubes (CNTs) can propagate waves of the order of terahertz (THz). THz waves in nanoscale materials and nano-photonic or nano-phononic devices have opened a new topic on the wave characteristics of nanomaterials[4,5,6]. They also have applications in CNTs and other applications [7,8,9]. As dimensions of the material become smaller, however, their resistance to deformation is increasingly determined by internal or external discontinuities (such as surfaces, grain boundary, strain gradient, and dislocation). Although many sophisticated approaches for predicting the mechanical properties of nanomaterials have been reported, few addressed the challenges posed by interior nanostructures such as the surfaces, interfaces, structural discontinuities and deformation gradient of the nanomaterials under extreme loading conditions. The use of atomistic simulation may be a potential solution in the long run. However, it is well known that the capability of this approach is much limited by its need of prohibitive computing time and an astronomical amount of data generated in the calculations. Wave propagation analysis using continuum models, especially using non-local elasticity models can used to address the above problems.

Wave propagation studies mainly include the estimation of wavenumber and wave speeds such as phase and group speeds. The concept of group velocity may be useful in understanding the dynamics of carbon nanotubes, since it is related to the energy transportation of wave propagation. The primary objective of this paper is to study the wave propagation in nanostructures, so as to examine the effect of length scales on the wave dispersion from the viewpoint of group velocity or energy transportation. To describe the effect of microstructures of a nanostructures on its mechanical properties, it is assumed that the model of the nanostructure is made of a kind of non-local elastic material, where the stress state at a given reference location depends not only on the strain of this location but also on the higher order gradient of strain, so as to take the influence of the microstructures into account. It is reported that both local elastic models (where effects of nano scale is not considered) and non-local elastic models (where the effect of scale is considered) can offer the correct prediction when the wavenumber is on the lower side. However, the results of the elastic model remarkably deviate from those given by the non-local elastic model with an increase in the wavenumber [10]. As a result, the microstructures play an important role in the dispersion of waves in nanoscale structures. Since terahertz physics of nanoscale materials and devices are the main concerns in wave characteristics of nanostructures such as CNTs, the small-scale effect must be of significance in achieving accurate dispersion relations as the wavelength in the frequency domain is in the order of nanometers.

Since controlled experiments at the nanoscale are difficult, and with atomistic simulation being computationally expensive, continuum modeling can prove to be very valuable in the advancement of nanoscale structures. In view of growing interest in terahertz vibrations and waves of nanoscale materials and devices, it is relevant to systematically study terahertz wave propagation in individual nanostructures. Since terahertz physics of nanoscale materials and devices are major concerns for nanostructure's wave characteristics, small-scale effect needs be considered in the mathematical models (especially the continuum models) as the wavelength is normally of the order of nano meter.

This paper is organized as follows. First, the non-local gradient elasticity theories are introduced. Then the wave characteristics in 1-D nanostructures such as nano rods, beams and 2-D nano structures such as the monolayer Graphene are studied next. Some interesting numerical examples are presented to bring out the essential features of wave characteristics in these structures. The paper ends with some important conclusions.

2. THEORY OF GRADIENT ELASTICITY

The every matter in this world is composed of atoms moving under the influence of their mutual inter-atomic forces. These interactions at microscopic scale are the physical origin of many macroscopic phenomena. Atomistic investigation helps to identify macroscopic properties and their correlations, which enhances understanding of various physical theories. There are many micro- continuum theories (which is normally referred to as Gradient Elasticity theories) proposed to understand the behavior of materials at the atomistic scales. The fundamental difference between the micro-continuum theories from the classical continuum theories is that, in the former, the microstructure properties are embedded within the framework of continuum theory or in other words, it is a nonlocal continuum model to describe the long-range material interaction. This extends the application of the continuum model to microscopic space and problems involving short-time scales.

Next we will to address the need for gradient elasticity theories. In the atomistic regimes, the experimental evidence and observations with newly developed devices such as atomic force microscopes have suggested that classical theory of elasticity is not sufficient for an accurate and detailed description of the deformation phenomena at the nanometer scales. More notably size effects could not be captured by theory of elasticity. Moreover, in the classical theory of elasticity, due to the assumption of point-to-point correspondence of stresses and strains, the elastic singularities arising due to application of point loads or occurring at dislocation lines and crack tips cannot be removed, and the same is true for discontinuities occurring at interfaces.

The length scales of a material at atomistic scales are often sufficiently small, and hence for the applicability of classical continuum models, we need to consider the small length scales such as lattice spacing between individual atoms, grain size, etc. Although solution through molecular dynamics (MD) simulation is a possibility for such problems, its large computational cost prohibits its use for a general analysis. The conventional continuum models cannot handle scale effects. Hence the best alternative is to use those methods, which provide the simplicity of continuum models and at the same time incorporate the effects of scale in such chosen continuum models. This is done through the use of gradient elasticity theory. Here, we assume that stresses to depend on the strains not only at an individual point under consideration, however at all points of the body. In this theory, the internal size or scale could be represented in the constitutive equations simply as material parameters. Such a nonlocal continuum mechanics model has been widely accepted and has been applied to many problems including wave propagation, dislocation, crack problems, etc.[11]

2.1 Eringen's Stress Gradient Theory

Eringen's Stress Gradient Theory (ESGT) of elasticity assumes an equivalent effect due to nearest neighbor interaction and beyond the single lattice in the sense of lattice average stress and strain. In this theory, it is assumed that the stress state at any reference point given by coordinates $x = (x_1, x_2, x_3)$ in the body is assumed to be dependent not only on the strain state at this point, but also on the strain states at all other neighboring points given by coordinate vector $\boldsymbol{x}'$ of the body. This is in accordance with atomic theory of lattice dynamics and experimental observations on phonon dispersion. The most general form of the constitutive relation in the nonlocal elasticity type representation involves an integral over the entire region of interest. The integral contains a nonlocal kernel function, which describes the relative influences of the strains at various locations on the stress at a given location. The constitutive equations of linear, homogeneous, isotropic, non-local elastic solid with zero body forces are given by [12]

$$\sigma_{kl,k} + \rho(f_l - \ddot{u}_l) = 0 \tag{1}$$

where

$$\begin{aligned} \sigma_{kl}(x) &= \int_{\Omega} \alpha\left(\left|x - x'\right|, \xi\right) \sigma^{c}_{kl}(x') \, d\Omega(x') \\ \sigma^{c}_{kl}(x') &= \lambda_{rr}(x')\delta_{kl} + 2\mu\varepsilon_{kl}(x') \\ \varepsilon_{kl}(x') &= \frac{1}{2}\left(\frac{\partial u_k(x')}{\partial x_l'} + \frac{\partial u_l(x')}{\partial x_k'} \right) \end{aligned} \tag{2}$$

Eqn. (1) is the equation of equilibrium, where σ_{kl}, ρ, f_l and $\boldsymbol{u_l}$ are the stress tensor, mass density, body force density and the displacement vector at a reference point x in the body, respectively, at time t. Eqn. (2) is the classical constitutive relation where $\boldsymbol{\sigma^{c}_{kl}(x')}$ is the classical stress tensor at any point $\boldsymbol{x}'$ in the body, which is related to the linear strain tensor $\boldsymbol{e_{kl}(x')}$ at the same point through the Lame´ constants $\boldsymbol{\lambda}$ and $\boldsymbol{\mu}$. Eqn. (2) is the classical strain-displacement relationship. The only difference between the above three equations in Eqns. (2) and the corresponding equations of classical elasticity is the introduction of first of the Eqn.(2), which relates the global (or nonlocal) stress tensor $\boldsymbol{\sigma_{kl}}$ to the classical stress tensor $\boldsymbol{\sigma^{c}_{kl}(x')}$ using the modulus of nonlocal ness. The nonlocal modulus $\boldsymbol{\alpha(|x - x'|, \xi)}$ is the kernel of the integral in the first of Eqn. (2) and contains parameters which correspond to the nonlocal parameter [13]. A dimensional analysis of first of the Eqn. (2) clearly shows that the nonlocal modulus has dimensions of $(\text{length})^{-3}$ and hence it depends on a characteristic length ratio $\boldsymbol{a/l}$, where $\boldsymbol{a}$ is an internal characteristic length (lattice parameter, size of grain, granular

distance) and $\boldsymbol{l}$ is an external characteristic length of the system (wavelength, crack length, size or dimensions of sample)[14], $\boldsymbol{\Omega}$ is the region occupied by the body. Therefore the nonlocal modulus can be written in the following form:

$$\alpha = \alpha\left(\left|x - x'\right|, \xi\right), \ \xi = \frac{e_0 a}{l} \tag{3}$$

where $\boldsymbol{e_0}$ is a constant appropriate to the material and has to be determined for each material independently[14].

After making certain assumptions[14], the integro-partial differential equations of the stress gradient theory can be simplified to partial differential equations. For example, first of Eqn. (2) takes the following simple form:

$$\left(1 - \xi^2 l^2 \nabla^2\right)\sigma_{kl}(x) = \sigma_{kl}^c(x) = C_{klmn}\varepsilon_{mn}(x) \tag{4}$$

where C_{ijkl} is the elastic modulus tensor of classical isotropic elasticity and ε_{ij} is the strain tensor. where ∇ denotes the second order spatial gradient applied on the stress tensor $\sigma_{kl,k}$ and $\xi = e_0 l / a$. The validity of Eqn. (4) is established by comparing the expressions for frequency of waves from the above ESGT model with those of the Born-Karman model of lattice dynamics[14]. Eringen reports a maximum difference of 6% and a perfect match for nonlocal constant value of $\boldsymbol{e_0}$ = 0.39[14]. Eqn.(4) on simplification will yield the following constitutive equations for 1-D and 2-D problems is given by

$$\begin{aligned}
&\sigma_{xx} - (e_0 a)^2 \frac{d^2\sigma_{xx}}{dx^2} = E\varepsilon_{xx} \\
&\sigma_{xx} - (e_0 a)^2\left[\frac{d^2\sigma_{xx}}{dx^2} + \frac{d^2\sigma_{xx}}{dy^2}\right] = \frac{E}{1-\nu^2}\left(\varepsilon_{xx} + \nu\varepsilon_{yy}\right), \ \sigma_{yy} - (e_0 a)^2\left[\frac{d^2\sigma_{yy}}{dx^2} + \frac{d^2\sigma_{yy}}{dy^2}\right] = \frac{E}{1-\nu^2}\left(\varepsilon_{yy} + \nu\varepsilon_{xx}\right) \\
&\tau_{xy} - (e_0 a)^2\left[\frac{d^2\tau_{xy}}{dx^2} + \frac{d^2\tau_{xy}}{dy^2}\right] = \frac{E}{2(1+\nu)}\gamma_{xy}
\end{aligned} \tag{5}$$

where all the σ s and τ have usual meaning.

2.2 Strain Gradient Theory

As mentioned earlier there are many strain gradient theories reported in the literature. The most notable of them is the Mindlin theory[15] formulated in 1964. This theory's constitutive model gives a total of 1764 coefficients in the constitutive matrix out of which 903 are independent. Even for isotropic material assumption, the number of independent constants to be determined is equal to 18. It is indeed a daunting task to determine them and hence, this theory, although is rich in completeness and theoretical basis, has very little practical use. Hence, in order to increase its utility and reduce the number of constants to be determined, many researchers including Mindlin have made series of assumptions on deformation field of the microstructure and many such theories have been reported in the literature. For wave propagation analysis, we need a simple theory that not only has less number of constants in the constitutive model, but also is stable. That is, one of the problems associated with the strain gradient theories is that in some theories, the governing differential equations are such that they give unstable or divergent solutions (see[16]] for more details on stability issues associated with strain gradient theories). Hence, in this paper, we will outline a very simple strain gradient theory that can provide good insight into propagation of waves in nanostructures. One such theory is the Laplacian based *Strain Gradient Theory*.

Laplacian based strain gradient theories are extensively used in static analysis, especially in those structures involving cracks, primarily to overcome the effects of stress singularities near the crack tips. However its use in dynamic analysis is quite different, where it is primarily used to describe the dispersive wave propagation in a heterogeneous media. Laplacian based strain gradient theory can be derived using simple lattice model consisting of springs and masses shown in Fig 3.

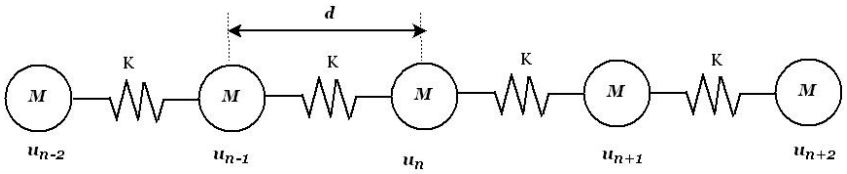

Figure 3. 1-D discrete lattice model

The figure shows the deformation of the 1-D lattice at discrete points ***n+2, n+1, n,n-1,n-2, ...*** Let us consider the 3 particles in this lattice at points ***n,n-1, and n+1***. If we isolate these points, draw the free body diagram and apply Newton's second law, we get

$$M\ddot{u}_n = K(u_{n+1} - u_n) + K(u_{n-1} - u_n) = K(u_{n+1} - 2u_n + u_{n-1}) \tag{7}$$

Next, we will convert this discritized equation motion into a continuum equation. For this, we will expand the deformation of the $\boldsymbol{n+1}$ and $\boldsymbol{n-1}$ particles having a spacing d between them in Taylor's series as

$$u_{n-1} = u_n - d\frac{du_n}{dx} + d^2\frac{1}{2}\frac{d^2u_n}{dx^2} - \ldots\ldots, \quad u_{n+1} = u_n + d\frac{du_n}{dx} + d^2\frac{1}{2}\frac{d^2u_n}{dx^2} + \ldots\ldots \tag{8}$$

We assume that homogenized lattice has a Young's modulus E and density ρ and they can be expressed in terms of the lattice spacing constant K and lattice mass M as $\boldsymbol{E = Kd/A}$ and $\boldsymbol{M = \rho Ad}$, where A is the area of the equivalent continuum and d is the spacing of particles in the lattice. Using Eqn. (8) in Eqn. (7) and ignoring the higher order terms in the Taylor series and assuming $\boldsymbol{u_n = u(x, t)}$, we get

$$E\left(\frac{d^2u}{dx^2} + \frac{1}{12}d^2\frac{d^4u}{dx^4}\right) = \rho\frac{d^2u}{dt^2} \tag{9}$$

The equation above can be re-written as

$$E\frac{d}{dx}\left(\varepsilon + \frac{1}{12}d^2\frac{d^2\varepsilon}{dx^2}\right) = \rho\frac{d^2u}{dt^2} \tag{10}$$

From the equation above, one can easily recognize that the left hand represents the constitutive model of the strain gradient theory and can be written as

$$\sigma = E\left(\varepsilon + \frac{1}{12}d^2\frac{d^2\varepsilon}{dx^2}\right) \tag{11}$$

The equation above represents the constitutive model for a 1-D case and this equation can be generalized to the 3-D case as

$$\sigma_{ij} = C_{ijkl}\left(\varepsilon_{kl} + g^2\frac{d^2\varepsilon_{kl}}{dm^2}\right) \tag{12}$$

where g is the length scale parameter, which is normally expressed in terms of lattice parameter d and C_{ijkl} is the fourth order tensor. The constitutive model given in Eqn. (12) has been proposed by a number of researchers[17,18]. The main problem with the above constitutive models is that the final solutions provided by certain order of this constitutive model are neither unique nor stable. For example, the constructive model for the second order strain gradient mode of 1-D nanorod, which is given by

$$\sigma(x) = E\left(\varepsilon(x) + g^2 \frac{d^2 \varepsilon_x}{dx^2} \right) \tag{13}$$

is shown to be unstable (see[10]), while the fourth order strain gradient model of the same nanorod, whose constitutive model is given by

$$\sigma(x) = E\left(\varepsilon(x) + g^2 \frac{d^2 \varepsilon_x}{dx^2} + g^4 \frac{d^4 \varepsilon_x}{dx^4} \right) \tag{14}$$

is found to be highly stable. However, Aifantis and his coworkers[19,20] derived the second order strain gradient elasticity constitutive model as

$$\sigma_{ij} = C_{ijkl}\left(\varepsilon_{kl} - g^2 \frac{d^2 \varepsilon_{kl}}{dm^2} \right) \tag{15}$$

Note that the main difference between Eqn. (13) and Eqn. (15) is that the negative sign before the higher order strain terms. The above models said to be highly stable. The sign of the gradient term and the issues of uniqueness and stability as opposed to their ability to describe dispersive wave propagation have opened up serious debates across the elasticity community; for example, see for instance the early study of Mindlin and Tiersten[21] and Yang and Gao[22] where this dilemma was aptly named as *sign paradox*

3. WAVE PROPAGATION IN 1-D MODELS

In this section, we will discuss the wave propagation characteristics of three different 1-D models, namely the Stress gradient Rods, Strain Gradient rods and Stress gradient beams.

3.1 Eringen's Stress Gradient Nano Rod:

The first step in performing wave propagation analysis is to obtain the governing differential equation. Rods can sustain only the longitudinal motion along the axis of the nanorod system and hence the deformation field can be written as $u(x,y,z,t) = u(x,t)$. Using the constitutive model given by Eqn. (5) and theory of elasticity principle, one can write the governing differential equation for a stress gradient nanorod as

$$EA\frac{\partial^2 u}{\partial x^2} + (e_0 a)^2 \rho A \frac{\partial^4 u}{\partial x^2 \partial t^2} = \rho A \frac{\partial^2 u}{\partial t^2} \tag{16}$$

The first step in determining the wavenumber and group speeds is to first transform Eqn. (16) to frequency domain using Discrete Fourier Transform (DFT) using the transformation given by

$$u(x,t) = \sum_{n=1}^{N} \hat{u}(x,\omega) e^{i\omega t} \tag{17}$$

where N is the number of FFT points with ω as circular frequency. Here $i = \sqrt{-1}$. Substituting Eqn. (17) in Eqn. (16), the original PDE will be reduced to a set of ODEs, which are of constant coefficient type, whose solution will be of the form $\hat{u}(x,\omega) = Ae^{ikx}$, where k is the wavenumber, which requires to be computed. Substituting the assumed constant coefficient solution in the reduced set of ODEs, we get the characteristic equation for computation of wavenumber, which is given by

$$-k^2 + (e_0 a)^2 \eta^2 \omega^2 k^2 + \eta^2 \omega^2 = 0 \tag{18}$$

where $\eta = \sqrt{\rho / E}$. Solution of Eqn. (18) will yield

$$k_{1,2} = \pm\sqrt{\frac{\eta^2\omega^2}{1-(e_0a)^2\eta^2\omega^2}} \tag{19}$$

The wave frequency is a function of wavenumber *k,* the nonlocal scaling parameter e_0a and the material properties (E & ρ) of the nanorod. If e_0a = 0, the wavenumber is directly proportional to wave frequency, which will give a non-dispersive wave behavior. The cut-off frequency of this nanorod is obtained by setting $k = 0$ in the dispersion relation (Eqn. (18)). For the present case, the cut-off frequency is zero, that is, the axial wave starts propagating from zero frequency. The wavenumber as a function of nonlocal scale parameter e_0a is shown in Fig.4. From this figure, one can observe that at certain frequencies, the wavenumber is tending to infinity and value of this frequency, which is called the escape frequency, decreases with increase in the scale parameter. Its value can be analytically determined by looking at the wavenumber

$$\omega_{escape} = \frac{1}{(e_0a)\eta} = \frac{1}{(e_0a)}\sqrt{\frac{E}{\rho}} \tag{20}$$

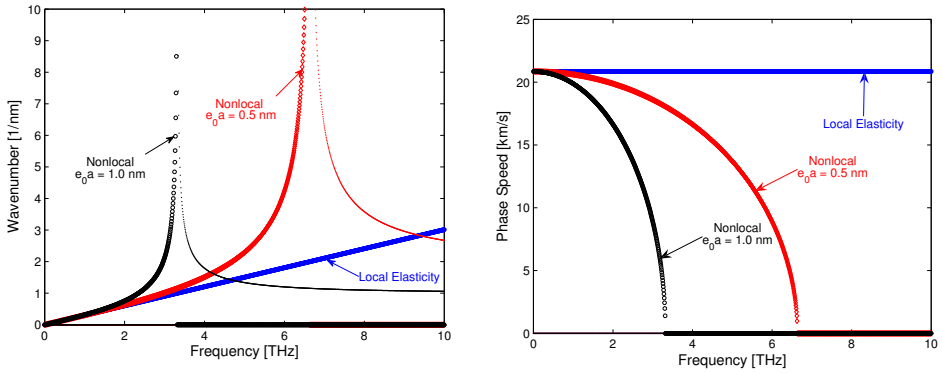

(a) (b)

Figure 4. Dispersion relations for Eringen's Nano Rods (a) Wavenumber relations (b) Group Speeds

The escape frequency is inversely proportional to the nonlocal scaling param-eter and is independent of the diameter of the nanorod. The variation of the escape frequency with nonlocal scaling parameter is shown in Fig. 4(a). Next, we will compute the wave speeds, namely the phase speeds and the group speeds, whose expressions are given by

$$C_P = \frac{\omega}{k} = \frac{1}{\eta}[1-(e_0a)^2\eta^2\omega^2]^{1/2},\ C_g = \frac{d\omega}{dk} = \frac{1}{\eta}[1-(e_0a)^2\eta^2\omega^2]^{3/2} \tag{21}$$

We see from Eqn. (21) that both phase and group speeds depend on the non-local parameter and the speeds depend on the frequency indicating the dispersiveness of the waves. When $e_0a \to 0$, we obtain the local rod solution, that is $C_p = C_g = 1/\eta = \sqrt{E/\rho}$. For the present analysis, a SWCNT is assumed as a nanorod. The values of the radius, thickness, Young's modulus and density are assumed as *3.5 nm, 0.35 nm*, *1.03 TPa*, and 2300 kg/m^3, respectively. Fig. 4(a) shows the variation of the axial wavenumber of a nanorod. The thick lines represent the real part and the thin lines show the imaginary part of the wavenumbers. From the figure, for a nanorod, it can be seen that there is only one mode of wave propagation that is, the axial or the longitudinal. For local or classical model, the wavenumbers for the axial mode has a linear variation with the frequency, which is in the THz range. The linear variation of the wavenumbers denotes that the waves will propagate non-dispersively. On the other hand, the wavenumbers obtained from nonlocal elasticity have a non-linear variation with the frequency, which indicates that the waves are dispersive in nature. However, the wavenumbers of this wave mode have a substantial real part starting from the zero frequency. This implies that the mode starts propagating at any excitation frequency and does not have a cut-off frequency. At the escape frequency, which was defined earlier, the wavenumbers tends to infinity as shown in Fig. 4(a). Hence, the nonlocal

elasticity model shows that the wave will propagate only up to certain frequencies and after that the wave will not propagate.

From Eqn. (21), we see that escape frequency are purely the function of non-local scaling parameter. From Eqn. (20), we see that as the value of $e_0 a$ increases, the numerical value of escape frequency decreases. Fig. 4(b) shows the variation of phase speeds with frequency. We can clearly see the shifting of the dispersion curves with the increase in the non-local parameter. In addition, one can see the extent of non-dispersiveness of waves in Eringen's nano rods.

3.2 Strain Gradient Nano Rod:

Using the constitutive equations given by Eqn. (13) and (14), we can write the governing equations for the second and fourth order strain gradient rods as

$$EA(e_0 a)^2 \frac{\partial^4 u}{\partial x^4} + EA\frac{\partial^2 u}{\partial x^2} - \rho A\frac{\partial^2 u}{\partial t^2} = 0 \tag{22}$$

$$EA(e_0 a)^4 \frac{\partial^6 u}{\partial x^6} + EA(e_0 a)^2 \frac{\partial^4 u}{\partial x^4} + EA\frac{\partial^2 u}{\partial x^2} - \rho A\frac{\partial^2 u}{\partial t^2} = 0 \tag{23}$$

From the equations above, the spatial order of the governing equations has increased from two in local model to four in second order strain gradient model and six in the fourth order model. Let us first consider the second order strain gradient model. Following the procedure outlined in the previous section, we can write the characteristic equation for wavenumber computation as

$$(e_0 a)^2 k^4 - k^2 + \eta^2\omega^2 = 0 \tag{24}$$

Fourth order equation in spatial direction will yield four wave modes (2 incident waves and the rest reflected wave components). The corresponding phase speed and group speeds can be written as

$$C_P^S = \frac{\omega^S}{k} = \frac{1}{\eta}\sqrt{1-(e_0 a)^2 k^2},\ C_g^S = \frac{d\omega^s}{dk} = \frac{1-2(e_0 a)^2 k^2}{\eta(1-(e_0 a)^2 k^2)} \tag{25}$$

As before in the case of Eringen's rod case, one can see that we can recover local rod solution by substituting $e_0 = 0$ .We will next compute one of the important feature of wave propagation of Second order SGT nanorods, which is its *Critical Wavenumber*, which is the wavenumber at zero frequency, which can be obtained from Eqn. (24) and its expression can be written as

$$k_{cr} = \pm\frac{1}{\sqrt{e_0 a}} \tag{26}$$

which is inversely proportional to the non-local parameter. As mentioned earlier, this rod will yield no-unique unstable solution (see [10] for details). Next we will derive the dispersion relation for the fourth order strain gradient model, which is given by

$$-(e_0 a)^4 k^6 + (e_0 a)^2 k^4 - k^2 + \eta^2\omega^2 = 0 \tag{27}$$

Corresponding phase and group speed expressions can be written be as

$$C_P = \frac{\omega}{k} = \frac{1}{\eta}\sqrt{1-(e_0 a)^2 k^2 + (e_0 a)^4 k^4},\ C_g = \frac{d\omega}{dk} = \frac{1-2((e_0 a)^2 k^2[1-(e_0 a)^2 k^2]}{\eta\{1-(e_0 a)^2 k^2[1-(e_0 a)^2 k^2]\}} \tag{28}$$

Next, we will next plot the wavenumber and speeds with respect to the frequency. Such plots are generated using the diameter (*d*), Young's modulus (*E*) and density (ρ) are assumed as 5 *nm*, 1.06 *TPa*, and 2270 kg/m^3, respectively. The wavenumber relations are generated for $e_0 a = 0.2$ and it is shown in Fig 5.

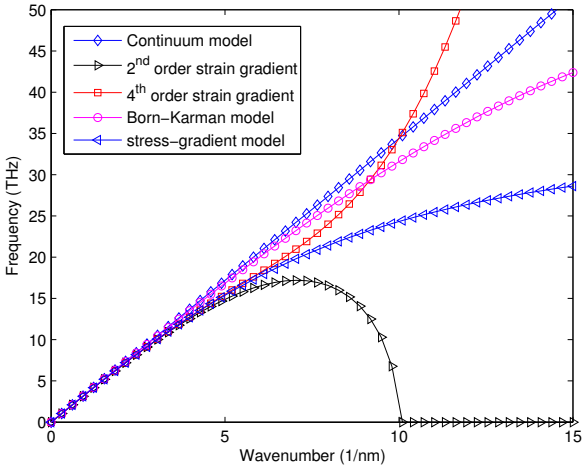

Figure 5. Wavenumber relations for Strain gradient Nano Rods

The waves in both second and fourth order strain gradient are non-dispersive unlike local rod. It can also be seen that the fourth-order strain gradient model give improved approximation over the second order strain gradient model, as compared to the classical continuum model. They are also compared with the results are of the Born-Karman model[23] (atomistic model) and the Eringen's nano rod model presented previously.The instability of the Second order SGT model can be seen developing in Fig. 5 for wavenumbers larger than $1/\sqrt{e_0 a}$, where the angular frequency and the phase velocity become imaginary. This means that the waves with larger wavenumbers (or, equivalently, with smaller wavelengths) cannot propagate through this medium. Instead, the imaginary frequency and velocity imply that the response occurs everywhere in the medium instantaneously. This is physically unrealistic. Therefore, these smaller wavelengths should not be considered. Filtering shorter waves occurs automatically in a discrete medium, where wavelengths smaller than two times the particle size cannot be monitored. However, in a continuous medium, all wavelengths can in principle be present. Especially when shock waves are investigated, the loading triggers waves with all wavelengths. The imaginary angular frequency (or phase velocity) of these high-frequency waves prohibits a proper wave propagation simulation with this model. The cut-off value for the wavenumber occurs at $k = 1/\sqrt{e_0 a}$ (see Fig. 5). In the response of the Fourth order strain gradient model, the effect of these high frequency waves are of minor importance. In summary, the wave behavior of the Second order strain gradient model and Fourth order models are quite different and in addition, instability in the second order model can be clearly seen.

3.3 Stress Gradient Nano Beam:

In this section we will derive the governing differential equation for a stress gradient nano rods. The beam deformation field is based on Euler-Bernoulii beam theory and is given by

$$u(x,y,z,t) = u^0(x,t) - z\frac{\partial w}{\partial x},\ w(x,y,z,t) = w(x,t) \tag{29}$$

where w and u^0 are the transverse and axial displacements of the point $(x,0)$ on the middle plane (that is, $z = 0$) of the beam, where z is the thickness coordinate. The only nonzero strain of the Euler-Bernoulli beam theory, accounting for the strain is the axial strain given by

$$\varepsilon_{xx} = \frac{\partial u}{\partial x} = \frac{\partial u^0}{\partial x} - z\frac{\partial^2 w}{\partial x^2} \tag{30}$$

Using the constitutive model given in Eqn. (5) and the theory of elasticity procedure, we get the following governing equation do stress gradient rod, which is given by

(31)

$$EI\frac{\partial^4 w}{\partial x^4}+\rho A\frac{\partial^2 w}{\partial t^2}-\rho A(e_0 a)^2\frac{\partial^4 w}{\partial x^2\partial t^2}$$

we can clearly see that when $e_0 a$ =0, we recover the governing equation of the local Euler Bernoulli beam.

Next, we will transform Eqn. (31) to frequency domain using DFT and this procedure will transform the Governing PDE to a set of ODEs, which will again be constant coefficient type. Adopting the same procedure as was done for nano rods, we get the following characteristic equation for wavenumber computation, which is given by

$$EIk^4-\rho A\omega^2(e_0 a)^2k^2-\rho A\omega^2=0 \tag{32}$$

Fourth order equation will give four modes, two of which are forward moving wave modes, while the other two correspond to backward moving or reflected wave components. Solving Eqn. (32), we get

$$k_{1,2,3,4}=\pm\sqrt{\frac{\rho A\omega^2(e_0 a)^2\pm\sqrt{\rho A\omega^2(4EI+\rho A\omega^2(e_0 a)^4}}{2EI}} \tag{33}$$

From the above equation, we can see that unlike Eringen's nano rod, the Eringen's nano beam does not exhibit any escape frequency and in addition, cut-off frequency also does not exist for this kind of beam. The phase speed can be calculated from $C_p=\omega/k$. The expression for group speed is given by

$$C_g=\frac{2EIk_\alpha^3+\rho A(e_0 a)^2k_\alpha}{\rho A\omega(1+(e_0 a)^2k_\alpha^2)} \tag{34}$$

where k_α =1,2,3,4 corresponding to four wave modes . From this expression we can plot the dispersion relation. This plot will give full description of the wave propagation in beams. Both the speeds are also a function of nonlocal scaling parameter and wave circular frequency.

The spectrum curves (wavenumber vs. frequency) and dispersion curves (group speed vs. frequency) are shown for both local and nonlocal continuum models in Fig. 6 (a) and Fig. 6 (b).

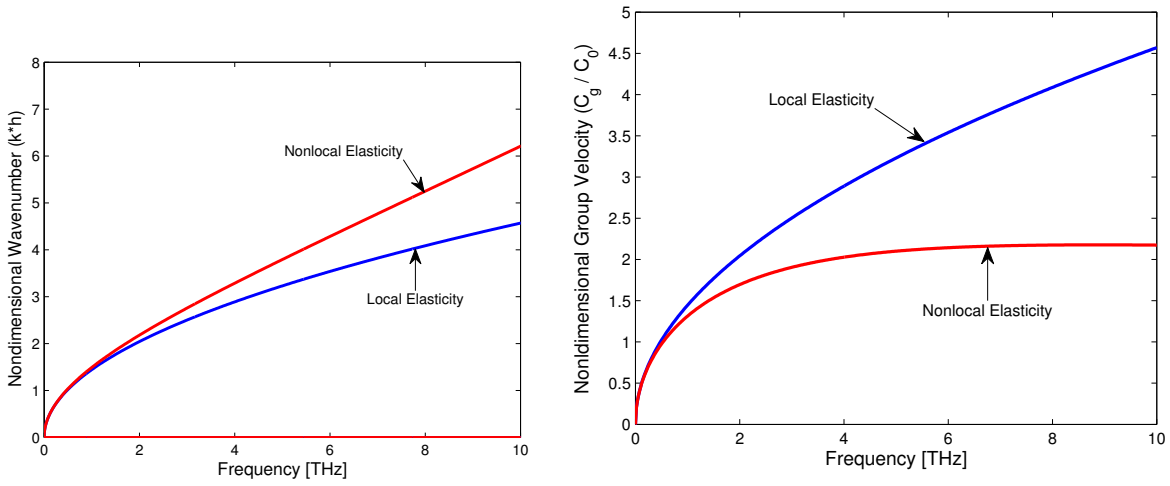

(a) (b)

Figure 6. Wavenumber and dispersion relations for Stress gradient Nano beams

As mentioned earlier, the plot does not show the existence of escape or cut-off frequency and the behavior is pretty much the same as local beam solution. The main difference is that, the scale parameter changes the slope of the wavenumber

plot, which means substantial change in the group speeds as shown in Fig. 6(b). That is, introduction of scale parameter, reduces the group speeds in comparison with local Euler-Bernoulli beam.

4. WAVE PROPAGATION IN 2-D MODELS

Graphene are 2-D nanostructures and these structures, unlike CNTs, exhibit behavior in the two coordinate directions. That is, a load in the direction of one of the coordinates will give rise to deformations in both the coordinate directions. In wave propagation terminology, an incident wave in one of the coordinate directions will cause circularly crested waves that can be resolved in two coordinate directions. This means, there will be two different wavenumbers corresponding to two coordinate directions.

Although the existence of Graphene in different forms was known, there was difficulty in extracting its pristine form. For the first time, it was possible to isolate single two dimensional atomic layers of atoms[24]. These are among the thinnest objects imaginable. The strongest bond in nature, the C-C bond covalently locks these atoms in place giving them remarkable mechanical properties. A single layer of Graphene is one of the stiffest known materials characterized by a remarkably high Young's modulus of approximately *1 TPa* [25]. Graphene is a class of two-dimensional carbon nanostructure, which holds great promise for the vast applications in many technological fields. After the Graphene sheets were successfully extracted from graphite, the researchers have realized the volume of potential applications. It would be one of the prominent new materials for the next generation nano-electronic devices. Reports related to its applications as strain sensor, mass and pressure sensors, atomic dust detectors, enhancer of surface image resolution are reported in the literature. In addition, Graphene structures find application such as atomic-force microscopes, composite nano fibers, nano bearings and nano actuators, etc. Consequently interest is drawn towards research of Graphene in the field of physics, material science and engineering[26]. With the difficulty for the controlled experiments at the nanometer scale, the numerical simulation has been performed widely to understand the behavior of these structures. In this paper, we will use continuum modeling using non-local elasticity to model these 2-D nanostructures to understand the wave propagation behavior in these structures. The importance of size effects and need for non-local theories is not elaborated or emphasized again here and it is implicit that these effects are again important in the context of modeling 2-D nanostructures. Studies on wave propagation aspect of Graphene sheets available in literature are extremely scarce. Graphene sheets can have interesting waveguide properties at very high frequencies in the order of Tera-Hertz (THz), which is the subject of investigation of this section.

4.1 Governing Equations for Flexural Wave Propagation in Mono- layer Graphene Sheets

Graphene sheet is idealized as 2-D plate that is subjected to both in-plane and out-of-plane loading. As a result, the Graphene sheet can undergo both axial, bending and shear deformation. Fig. 7(a) shows a rectangular Graphene sheet and Fig. 7(b) shows its equivalent continuum model.

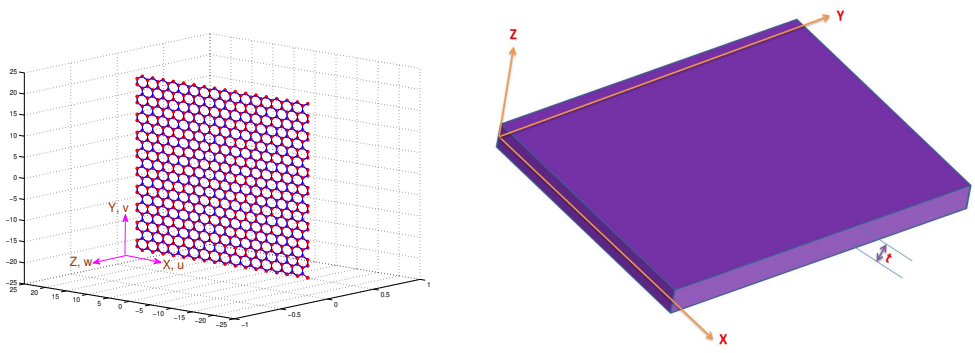

Figure 7. Single-layered Graphene sheet: (a) Discrete model (a monolayer Graphene of 40 ×40, consists of 680 carbon atoms arranged in hexagonal array) (b) Equivalent continuum model.

Here, the Graphene is treated as an isotropic plate. If $w(x,y,t)$ is the transverse displacement, the governing differential equation for such a structure considering Eringen's non-local model constitutive relations (Eqn.(6)) is given by (see [10] for more details)

$$C_{11}I_2\frac{\partial^4 w}{\partial x^4}+2(C_{12}+2C_{66})I_2\frac{\partial^4 w}{\partial x^2\partial y^2}+C_{22}I_2\frac{\partial^4 w}{\partial y^4}-J_0(e_0a)^2(\frac{\partial^4 w}{\partial x^2\partial t^2}+\frac{\partial^4 w}{\partial y^2\partial t^2})$$
$$+J_2(e_0a)^2(\frac{\partial^6 w}{\partial x^4\partial t^2}+2\frac{\partial^6 w}{\partial x^2\partial y^2\partial t^2}+\frac{\partial^4 w}{\partial y^2\partial t^2})+J_2\frac{\partial^2 w}{\partial t^2}-J_0{}^2(\frac{\partial^4 w}{\partial x^2\partial t^2}+\frac{\partial^4 w}{\partial y^2\partial t^2})=0 \quad (35)$$

where

$$C_{11}=C_{22}=\frac{E}{1-\nu^2},\ C_{12}=C_{21}=\frac{\nu E}{1-\nu^2},\ C_{66}=G=\frac{E}{2(1+\nu)}$$
$$I_2=\int_{-h/2}^{h/2}z^2dz,\ J_0=\int_{-h/2}^{h/2}\rho z\,dz,\ J_2=\int_{-h/2}^{h/2}\rho z^2dz$$

with E,ρ,ν and z being the Young's Modulus, density, Poisson's ratio and thickness coordinate, respectively.

4.2 Wave Dispersion Analysis:

The deformation field is transformed to frequency domain and it is assumed that the model is unbounded in $Y-$direction (although bounded in $X-$direction). Thus the assumed form is a combination of Discrete Fourier transforms in $Y-$direction and Fourier transform in time, which is written as

$$w(x,y,t)=\sum_{n=1}^{N}\sum_{m=1}^{M}\hat{w}(x)e^{-i\eta y}e^{i\omega_n t} \quad (36)$$

The ω_n and the η_m are the circular frequency at n^{th} sampling point and the wavenumber in $Y-$direction at the m^{th} sampling point, respectively. The N is the index corresponding to the Nyquist frequency in FFT, and $j=\sqrt{-1}$. Substituting Eqn.(36) in Eqn.(35), we get the following ODE

$$H_4\frac{d^4\hat{w}}{dx^4}+H_2\frac{d^2\hat{w}}{dx^2}+H_0\hat{w}=0 \quad (37)$$

where

$$H_4=C_{11}I_2-J_2(e_0a)^2\omega_n^2,$$
$$H_2=-2(C_{11}+2C_{66})I_2\eta_m^2+J_0(e_0a)^2\omega_n^2-2J_2(e_0a)^2\eta_m^2\omega_n^2+J_2\omega_n^2,$$
$$H_2=C_{22}I_2\eta_m^2-J_0(e_0a)^2\omega_n^2-J_2(e_0a)^2\eta_m^2\omega_n^2-J_0\omega_n^2-J_2\omega_n^2\eta_m^2$$

Since this is an ODE is having constant coefficients, its solution can be written as $\hat{w}(x)=\tilde{w}e^{ikx}$, where k is the wavenumber in the X−direction, yet to be determined and $\tilde{w}$ is an unknown wave coefficient. Substituting this assumed form of $\hat{w}(x)$ in the ODE gives for $\tilde{w}\neq 0$), we get the characteristic equation for computation of wavenumber as

$$H_4k^4+H_2k^2+H_0=0 \quad (38)$$

Solving the above equation, we get

(39)

$$k = \pm\sqrt{\frac{-H_2 \pm \sqrt{H_2^2 - 4H_0H_4}}{2H_4}}$$

Next, we compute the group speed $C_g = d\omega / dk$, which is given by

$$C_g = \frac{4H_4k^3 + 2H_2k}{G_4k^4 + G_2k^2 + G_0} \tag{40}$$

where

$$G_4 = -2J_2(e_0a)^2\omega_n,\ G_2 = 2J_0(e_0a)^2\omega_n - 4J_2(e_0a)^2\eta_m^2\omega_n + 2J_2\omega_n$$
$$G_0 = -2J_0(e_0a)^2\eta_m^2\omega_n - 2J_2(e_0a)^2\eta_m^2\omega_n - 2J_0\omega_n - 2J_2\omega_n\eta_m^2$$

From the above expressions, we see that both the group speeds and wavenumber are functions of Y-directional wavenumber and the non-local scale parameter.

Looking at Eqn. (37), the term H_0 indicates the possibility of a waveguide having cut-off frequencies. This is obtained by setting $k = 0$ in the dispersion relation (Eqn. (40)) that is, for the present case one can set $H_0 = 0$, which gives the cut-off frequency expression as

$$\omega_c = \sqrt{\frac{C_{22}I_2\eta_m^4}{(J_0 + J_2\eta_m^2)(1 + (e_0a)^2\eta_m^2}} \tag{41}$$

The cut-off frequency is directly proportional to the *Y*–directional wavenumber (η_m) and is also dependent on the nonlocal scaling parameter. For $\eta_m = 0$, the wavenumbers of the flexural wave mode have a substantial real part starting from the zero frequency, which implies that the mode starts propagating at any excitation frequency and does not have a cut-off frequency. For $\eta_m \neq 0$, the flexural wave mode, however, has a certain frequency band within which the corresponding wavenumbers are purely imaginary. Thus, the wave mode does not propagate at frequencies lying within this band. These wavenumbers have a substantial imaginary part along with the real part, thus these waves attenuate as they propagate.

Next, the term H_4 in Eqn. (37) indicates the possibility of a waveguide having escape frequencies. Its value can be analytically determined by looking at the wavenumber expression and setting $k \to \infty$. This accounts to setting the $H_4 = 0$, which gives

$$\omega_e = \frac{1}{e_0a}\sqrt{\frac{C_{11}I_2}{J_2}} \tag{41}$$

Next, we will investigate the relations derived above and plot the wave behavior in the monolayer Graphene sheet. For the present wave propagation analysis, the material properties of the Graphene are assumed as follows: Young's modulus $E = 1.06\ TPa$ and density $\rho = 2300\ kg/m^3$. The choice of effective wall thickness t of nanostructures such as CNT, Graphene, etc., is a long-standing issue in nano mechanics. One of the best approaches to estimate the thickness of CNT (that is, rolled Graphene sheet) is to model single-wall CNTs as linear elastic thin shells [27]. The shell thickness t is determined by fitting the atomistic simulation results of tensile rigidity and bending rigidity of single-wall CNTs. Such an approach gives the CNT thickness t much smaller than the graphite inter-layer spacing *0.34 nm*, ranging from *0.06* to *0.09 nm*. The scattered CNT thickness *0.06 – 0.09 nm* depends on the inter- atomic potential as well as simulation details. The thickness of the Graphene chosen here is equal to $t = 0.089\ nm$, obtained by Kudin et. al.[27] via *ab inito* computations. They defined the effective thickness of Graphene or CNTs as $t = \sqrt{12 \text{ x Bending regidity/Tension regidity}}$.

The flexural wavenumber dispersion with wave frequency in the Graphene s shown in Figs. 8 (a) and 8 (b), respectively, obtained from both local and ESGT theories. For the present analysis, the nonlocal scaling parameter is assumed as e_0a = *0.5 nm*.

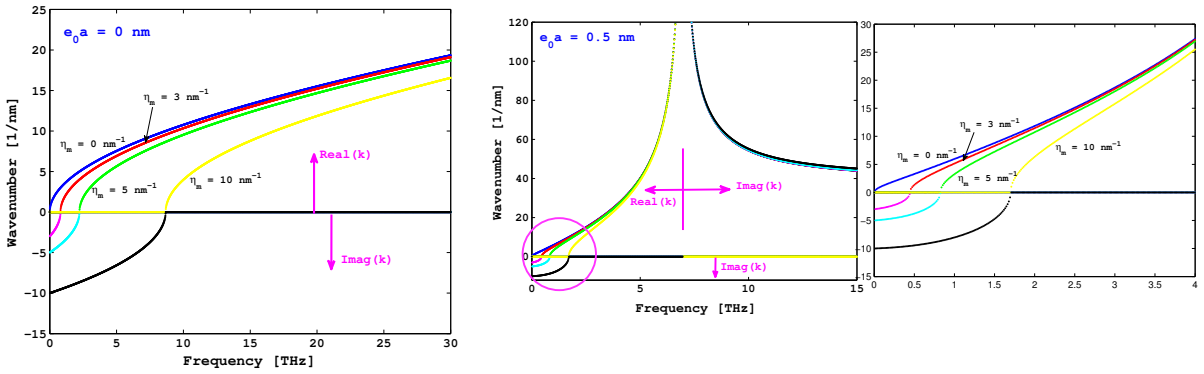

(a) (b)

Figure 8. Wavenumber dispersion in monolayer Graphene sheets (a) local elasticity (e_0a = *0 nm*) (b) Nonlocal elasticity (e_0a = *0.5 nm*). Wavenumber variation at lower frequencies is shown separately for clear visibility

The spectrum curves shown in Fig. 8(a) is for η_m = *0* (1D wave propagation), *3, 5, 10 nm*$^{-1}$. The local elasticity calculation shows that the flexural wavenumber follow a nonlinear variation at low values of wave frequency; and at higher frequencies, it varies linearly as shown in Fig. 8(a). This nonlinear variation indicates that the waves are dispersive in nature, that is, the waves will change their shape as they propagate. The linear variation indicates that the waves are in non-dispersive nature. For η_m = *0*, the wavenumbers of the flexural wave mode does not have a cut-off frequency. As η_m increases, all the waves are still dispersive in nature as shown in Fig. 8(a). As the *Y*−directional wavenumber increases from *0 to 10 nm*$^{-1}$, the wave modes are having a frequency band gap region, within which the corresponding wavenumbers are purely imaginary. Thus, the flexural mode does not propagate at frequencies lying within this band. Hence, these wavenumbers have a substantial imaginary part along with the real part, thus these waves attenuate as they propagate. It can also be seen that from Fig. 8(a), that the frequency band also increases with increase in η_m.

The wavenumber dispersion with frequency obtained from nonlocal elasticity (e_0a = *0.5 nm*) is shown in Fig. 8(b). The observations made in local elasticity are still valid in nonlocal elasticity also. The only difference is that, because of nonlocal elasticity, the wavenumbers of the flexural wave become highly non-linear and tends to infinity at escape frequency. It can be seen that the wavenumbers before escape frequency are real and after that imaginary. The cut-off frequency of the flexural wave for η_m = *3, 5 and 10 nm*$^{-1}$, respectively, occurs at *0.8087 THz, 2.2280 THz,* and *8.6820 THz* in local/classical elasticity, and at *0.4578 THz, 0.8392 THz,* and *1.7090 THz* in nonlocal elasticity (e_0a = *0.5 nm*). The nonlocal scale highly affects the frequency band gap of the flexural waves in Graphene sheet. The escape frequency of this flexural wave is *6.9580 THz* for e_0a = *0.5 nm*. It has also been observed that the escape frequencies are independent of η_m from Fig. 8(b).

5. CONCLUSIONS

This paper discusses the propagation of elastic waves in 1-D and 2-D nanostructures using gradient elastic models. Two different gradient elasticity models, namely the Erigen's Stress Gradient model and Mindlin's Strain Gradient models were discussed in this paper. Using this gradient elasticity models, waves in Nano rods, elementary beams and monolayer Graphene was analyzed. It was shown that, the scale parameter significantly changes the wave parameter as compared to local theory. The results show that the scale parameter introduces an escape frequency, beyond which no propagation takes place. The predicted results using non-local theories are shown to match very well with those predicted using atomistic simulation at fraction of a cost.

6. ACKNOWLEDGEMENTS

Author wishes to thank his former graduate student Mr S. Narendar for generating some results presented in this paper

REFERENCES

[1] Plimton, S. " Fast parallel algorithms for short range molecular dynamics" J. Comput Physics 117, 1-19 (1995)
[2] Hernaandez, C.M., Murray, T.W., S. Krishnaswarmy, S. "Photoacoustic characterization of the mechanical properties of thin films" Applied Physics Letters 80(4), 691-693 (2002).
[3] Philip, J., Hess, Feygelson, T., Butler, J.E., Chattopadhyay, S., Chen, K.H., and Chen, L.C. "Elastic mechanical and thermal properties of Nano crystalline diamond films" Journal of Applied Physics 93(4), 2164-2171 (2003).
[4] Ramprasad, R., and Shi, N., "Scalability of phononic crystal hetero structures" Applied PhysicsLetters 87, 111101 (2005).
[5] Sampathkumar, A., Murray, T.W., and Ekinci, K.L. "Photo thermal operation of high frequency nano electro mechanical systems" Applied Physics Letters 88, 223104 (2006).
[6] Schneider, D., Witke, T., Schwarz, T., Schoneich, B., and Schultrich, B. "Testing ultra-thin films by laser acoustics", Surface Coating Technology 126, 136-141 (2000).
[7] Sirtori, C. "Bridge for the terahertz gap" Nature 417, 132-133 (2002).
[8] Jeon, T., and Kim K. "Terahertz conductivity of anisotropic single walled carbon nanotube films", Applied Physics Letters 80, 34033405 (2002).
[9] Antonelli, G.A, and Maris H.J. "Pico second ultrasonics study of the vibrational modes of a nanostructure", Journal of Applied Physics 91, 32613267 (2002).
[10] Gopalakrishnan, S., and Narandar, S., [Wave Propagation in Nano Structures], Springer Verlag, London (2013)
[11] R. P. McNitt, R.P., Peddieson, J., and Buchanan, G.R. "Application of nonlocal continuum models to nanotechnology" International Journal of Engineering Science, 41, 305–312 (2003).
[12] Eringen, A.C. "On differential equations of nonlocal elasticity and solutions of screw dislocation and surface waves". Journal of Applied Physics, 54, 4703 (1983).
[13] Povstenko, Y.Z. "The nonlocal theory of elasticity and its applications to the description of defects in solid bodies" Journal of Mathematical Sciences, 97(1), 3840–3845 (1999).
[14] Eringen, A.C. "Linear theory of non-local elasticity and dispersion of plane waves" International Journal of Engineering Science, 10, 425–435 (1972).
[15] R.D. Mindlin, R.D. "Microstructure in linear elasticity" Archives of Rational Mechanical Analysis, 16, 51–78 (1964)
[16] Altan, B., and Aifantis, E. "On some aspects in the special theory of gradient elasticity" Journal of Mechanical Behavior of Materials, 8, 231– 282 (1997).
[17] Askes, H and Metrikine, A. "Higher-order continua derived from discrete media:continualisation aspects and boundary conditions" International Journal of Solids and Structures, 42, 187–202 (2005).
[18] Chang, C. and Gao, J. "Second-gradient constitutive theory for granular material with random packing structure" International Journal of Solids and Structures, 32, 2279–2293 (1995).
[19] Aifantis, E. "On the role of gradients in the localization of deformation and fracture" International Journal of Engineering science 30, 1279– 1299 (1992).
[20] Altan, B. and Aifantis, E. "On the structure of the mode iii crack-tip in gradient elasticity" Sripta Metallics and materials, 26, 319–324 (1992).
[21] Mindlin, R.D., and H. F. Tiersten, H.F. "Effects of couple stresses in linear elasticity" Archives of Rational Mechanical Analysis 11, 415–448 (1962).
[22] Yang, J and S. Guo, S. "On using strain gradient theories in the analysis of cracks" International Journal of Fracture 133, L19–L22 (2005).
[23] Ashcroft, N.W., and David, M.N. [Solid State Physics] Rinehart and Winston, New York (1976).
[24] Novoselov, K.S., and Geim, A.K. "Electric field effect in atomically thin carbon films" Science, 306(5696), 666–669 (2004).

[25] Poot, M. and van der Zant, H.S.J. “Nano mechanical properties of few layer Graphene membranes” Applied Physics Letters, 92, 6 (2008).
[26] Luo, X. and Chung, D.D.L. “Vibration damping using flexible graphite” Carbon, 38, 1510–1512 (2000).
[27] Kudin, K.N., Scuseria, G.E., and Yakobson, B.I. “C_2f, bn, and c nanoshell elasticity from *ab initio* computations” Physical Review B, 64, 235406 (2001).